Revista SAM N°1 – Año 2021

ISSN 1668-4788, N°1 (2021) p.01-06

Stability of the $Fe_{23}Zr_6$ phase in Zr alloys

Martín R. Tolosa* [1], María J. Jiménez[2], Pablo Pedrazzini[3], Constanza Arreguez[1], Lucas P. Acosta[1], Adrián Gómez[4], Marta S. Granovsky[5], Horacio Brizuela[1], Delia Arias[5], Nicolás Nieva[1]

(1) Laboratorio de Física del Sólido (LAFISO) – Instituto de Física del Noroeste Argentino (INFINOA) – Facultad de Ciencias Exactas y Tecnología – Universidad nacional de Tucumán (UNT) – CONICET, CP:4000, Tucumán, Argentina.
(2) Instituto de Física del Sur (IFISUR) – Departamento de Física – Universidad Nacional del Sur (UNS) – CONICET, CP:8000, Bahía Blanca, Argentina.
(3) Laboratorio de Bajas Temperaturas – Instituto Balseiro, Comisión Nacional de Energía Atómica Argentina, CONICET, CP:8400, San Carlos de Bariloche, Río Negro, Argentina.
(4) División Laboratorio de Materiales para la Fabricación de Aleaciones Especiales, Dpto. Tecnología de Aleaciones de Circonio, Comisión Nacional de Energía Atómica, CP:1804, Buenos Aires, Argentina.
(5) Instituto de Tecnología J. Sábato, Comisión Nacional de Energía Atómica Argentina, Universidad Nacional de San Martín, CP:1650, Buenos Aires, Argentina.

* e-mail: tolosamartinr@gmail.com

ABSTRACT

Alloyed with iron (Fe), niobium (Nb) and tin (Sn), zirconium (Zr) is the main element in the Zirlo-type alloys, vastly used as structural elements and as containers of burnable elements in nuclear reactors. Although Zr is a major component in this type of alloys, it is most important to know the phase diagrams of their components as well as possible. The binary phase diagram of the Fe-Zr system has been studied for some time now by several authors. However, in the Fe-rich region the existence of the $Fe_{23}Zr_6$ compound, which was first described in 1962, remains controversial. To clarify the origin of this phase, the present work deals with the manufacture and prolonged heat treatments at different temperatures of alloys located in the Fe-rich region of the Fe-Nb-Zr, Fe-Sn-Zr and Fe-Zr phase diagram. The experiments have been performed with raw materials whose degree of purity was varied. The phases present were identified by using X-ray diffraction (XRD), semi-quantitative microanalysis by using scanning electron microscopy analysis with energy dispersive spectrometry (SEM-EDS) and quantitative microanalysis by using electron microprobe with wavelength dispersive spectrometry (SEM-WDS). Finally, by using the results of characterization of heat-treated alloys for long annealing times at different temperatures, it is suggested that the presence of the $Fe_{23}Zr_6$ compound is an equilibrium phase of the Fe-Zr binary system.

Keywords: Zr alloys; Phase diagram; Nuclear materials.

INTRODUCTION

Zirconium-based alloys are widely used as fuel cladding in nuclear pressurized water reactors for their excellent mechanical properties, irradiation stability and resistance to corrosion. Alloyed with Fe, Nb and Sn, Zr is the main element in the Zirlo-type alloys, currently used as structural elements and as containers of burnable elements in nuclear reactors. Although Zr is a major component in this type of alloys, it is most important to know the phase diagrams of their components as well as possible.

The binary phase diagram of the Fe-Zr system has been extensively discussed in the literature and several assessments of the binary system have been published. At present, however, uncertainties and controversies about the existence of $Fe_{23}Zr_6$ compound still remain in the Fe-rich region of the Fe-Zr phase diagram.

The $Fe_{23}Zr_6$ phase was first described in 1962 by Svechnikov and Spektor [1] as a cubic phase. Then, Svechnikov et al. [2] noticed that this phase is a line compound and that the temperature of the $ZrFe_2 + L \rightarrow Fe_{23}Zr_6$ peritectic reaction is 1482ºC. After that, some authors confirmed its existence but other authors did not find the $Fe_{23}Zr_6$ phase. Arias et al. [3] suggested that the cause was probably that annealing times were not long enough. Granovsky and Arias [4] determined this phase exists at $Fe_{23}Zr_6$ stoichiometric composition. In 1996, Granovsky and Arias [5] reported the presence of this binary phase and suggested that $Fe_{23}Zr_6$ compound had a lattice parameter a = 1.168 (nm). They concluded that they could obtained this phase due to the fact that the cooling rates during the solidification of their ingots (15 g) were slower than those obtained by other authors. Then, Abraham et al. [6], who manufactured alloys of 15-20 g, confirmed the existence of this phase. However, in 2002, the $Fe_{23}Zr_6$ intermetallic compound was informed by Stein et al. [7] as a non-equilibrium phase of the binary system, and they suggested that this phase is an oxygen-stabilized compound, based on the observation of oxygen segregation by electron probe microanalyzer (EPMA).

Recently, studies in the Fe-rich corner on Fe-Nb-Zr [8, 9], Cu-Fe-Zr [10], Cr-Fe-Zr [11] and Fe-Sn-Zr [12-14] have again led to the discussion about the existence of this controversial phase. Authors of references [8-11] found the $Fe_{23}Zr_6$ phase, but in [12-14] it was not possible to detect it. Yang et al. [11], who found the $Fe_{23}Zr_6$ phase at 1200 ºC, discussed the stability of $Fe_{23}Zr_6$ by comparing the difference of the Gibbs energy of the system with and without this compound. They suggest that these two scenarios are highly competitive due to the small difference; so minor impurities or some kinetic factors can easily change the stability of this phase.

To clarify the $Fe_{23}Zr_6$ region of the Fe-Zr binary diagram, in the present work, a set of binary and ternary alloys were manufactured and subjected to a prolonged heat treatment at 800 ºC, 1100 ºC and 1200 °C.

MATERIALS AND METHODS

The raw materials of alloys designed to analyze the area of interest, which were labeled as M1, M2, M3 [15], J1, J2, H and L, are shown in Table 1. Buttons of alloys were prepared in an arc furnace with a non-consumable tungsten electrode and a water-cooled copper crucible, in a high purity argon atmosphere (at least 99.99%) by two different procedures: (1) The samples were melted by electric arc and solidified and cooled without electric arc presence; (2) The samples were melted by electric arc and solidified and cooled while an electric arc heated the sample, achieving in this way a slow cooling that lasted several minutes.

To reduce the contamination of oxygen, a Ti-50at.%Zr getter was melted prior to sample melting. The alloys were melted at least four times and turned upside down between each melting. No significant weight losses were registered. All samples were carefully cleaned, wrapped in tantalum sheets and placed in silica glass tubes previously cleaned and dried. After performing a vacuum better than 10^{-4} Pa, the tube was purged with high purity argon gas and sealed, keeping internal pressure of Ar. At the end of the heat treatment, the samples were quenched in water without breaking the seal. For the L binary alloy, a Ti-50at.%Zr getter was not used, the vacuum reached was about of 10^{-1} Pa and the tube was not purged with argon gas before sealing. Alloys H and L (both ~12 g) were manufactured with procedure (2) and alloys M1 to M3 (~7 g) and J1 (~12 g) to J2 (~8 g) with procedure (1). A summary of the manufacturing conditions is shown in Table 1.

Table 1: Degree of purity of the raw materials, procedures before the melting, mass and heat treatment of the samples.

Alloy	Degree of purity (wt%)	Use of Getter	Melting procedure	Mass [gram]	Tube sealing before heat treatment	Heat treatments [°C/hour]
M1, M2, M3	Fe (99.95 %) Zr (99.9 %, 600 ppm Fe and 200 ppm O) Nb (99.98 %)	Yes	(1)	7 g	Vacum 10^{-4} Pa, purged and sealed with Ar gas	800 °C / 3720 h
J1, J2	Fe (99.95%) Zr (99.9 %, 600 ppm Fe and 200 ppm O) Sn (99.999 %)	Yes	(1)	J1 - 12 g J2 - 8 g	Vacum 10^{-4} Pa, purged and sealed with Ar gas	1100 °C / 1440 h
H	Fe (99.95 %) Zr (99.9 %, 600 ppm Fe and 200 ppm O)	Yes	(2)	12 g	Vacum 10^{-4} Pa, purged and sealed with Ar gas	1200 °C / 10 h
L	Fe (99.95 %) Zr (99.8 %, 800 ppm Fe and 1200 ppm O)	No	(2)	12 g	Vacum 10^{-1} Pa, without Ar gas	1200 °C / 10 h

Before and after the heat treatments, the samples were prepared for characterization. For the quantitative microanalysis, samples were ground with Si carbide paper and polished with a cloth and diamond paste down to a particle size of 0.25 μm. Samples J1-J2 were chemically etched (with an aqueous solution of nitric and hydrofluoric acid) for metallographic inspection (with light and electron microscopy) and SEM-EDS analysis after the steps of grinding and polishing. X-ray analyses were made on polished samples radiating over an area of approximately 15 mm x 15 mm. Measurements were performed in the 20º–120° 2θ range using a Cu anode at room temperature. The phases present in as-cast and heat-treated alloys were identified by using metallographic techniques (optical microscope Olympus BX-60M), X-ray diffraction (XRD, PAN Analytical Empyrean diffractometer), scanning electron microscopy analysis with energy dispersive spectrometry (SEM-EDS, JEOL, Thermo and FEI INSPECT S50) and quantitative microanalysis by using electron microprobe with wavelength dispersive spectrometry (SEM-WDS microprobe JEOL JXA-8230).

RESULTS

A summary of the characterization results is shown in Table 2. The nominal composition of binary and ternary alloys is shown. The identified phases with crystal structure and chemical compositions of the samples heat-treated (HT) at 800 ºC, 1100 ºC, and 1200 ºC are indicated as well. Crystal structure was obtained from the results of XRD and the chemical compositions of SEM-WDS measurements.

Samples M1 to M3 HT at 800 ºC presented a three-phase field: the cubic Fe_2Zr(C15) and hexagonal $(Zr_{1-x}Nb_x)Fe_2$(C36) ternary Laves phases and the cubic Fe(α) [15]. All these ternary phases were also found by authors [8-9] at 1200 ºC and 700 ºC respectively.

Table 2: Nominal compositions of the alloys, characterization of the samples: phase identification, chemical composition (SEM-EDS and SEM-WDS), structure type and lattice parameters (XRD) in the 800 ºC, 1100 ºC, and 1200 ºC HT samples. When calculating was possible, the standard deviation of compositions was less than 0.3 at%.

Samples	Nominal Composition (at%)	Phases	Phase composition (at%)	Laticce parameters (Å)
M1	$Fe_{81}Nb_2Zr_{17}$	Fe(α) C15 C36$(Zr_{1-X}Nb_X)Fe_2$	$Fe_{98.7}Nb_{0.6}Zr_{0.7}$ $Fe_{71.4}Nb_{2.0}Zr_{26.6}$ $Fe_{72.4}Nb_{13.7}Zr_{13.9}$	a = 2.8699 a = 7.0155 a = 4.9363 c = 16.1509
M2	$Fe_{80}Nb_6Zr_{14}$	Fe(α) C15 C36$(Zr_{1-X}Nb_X)Fe_2$	$Fe_{98.8}Nb_{0.5}Zr_{0.7}$ $Fe_{71.4}Nb_{6.0}Zr_{22.6}$ $Fe_{72.3}Nb_{12.7}Zr_{15.0}$	a =2.8724 a =7.0101 a = 4.9146 c = 16.0393
M3	$Fe_{83}Nb_8Zr_9$	Fe(α) C15 C36$(Zr_{1-X}Nb_X)Fe_2$	$Fe_{98.5}Nb_{0.8}Zr_{0.7}$ $Fe_{71.5}Nb_{3.9}Zr_{24.6}$ $Fe_{72.5}Nb_{14.7}Zr_{12.8}$	a = 2.8656 a = 6.9247 a = 4.8610 c = 15.9770
J1	$Fe_{79.3}Zr_{20.7}$	Fe(α) C15	$Fe_{99.9}Zr_{0.1}$ $Fe_{71.7}Zr_{28.3}$	a = 2.870 a = 7.032
J2	$Fe_{92.0}Sn_{4.0}Zr_{4.0}$	Fe(α) C36	$Fe_{98.0}Sn_{1.9}Zr_{0.1}$ $Fe_{67.5}Sn_{14.2}Zr_{20.1}$	a = 2.882 a= 5.002 c= 16.200
H	$Fe_{79.3}Zr_{20.7}$	Fe(α) C15 $Fe_{23}Zr_6$	$Fe_{99.4}Zr_{0.6}$ $Fe_{72.7}Zr_{27.3}$ $Fe_{79.5}Zr_{20.5}$	a = 2.8778 a = 7.0599 a = 11.7384
L	$Fe_{79.3}Zr_{20.7}$	Fe(α) C15 $Fe_{23}Zr_6$	$Fe_{99.7}Zr_{0.3}$ $Fe_{72.8}Zr_{27.2}$ $Fe_{79.3}Zr_{20.7}$	a = 2.8747 a = 7.0547 a = 11.7609

The binary alloy J1 HT at 1100 ºC presented a two-phase field: the cubic Fe(α) phase and the cubic Fe_2Zr(C15) Laves phase. The Fe_2Zr(C15) binary phase, with $MgCu_2$ type cubic structure and lattice parameters a = 7.032 Å was also observed by other authors [1, 2, 4-7]. The ternary alloy J2 HT at 1100 ºC presented a field of two phases: the Fe(α) cubic phase and the hexagonal Fe_2Zr(C36) Laves phase. Figure 1 shows typical microstructure of samples J1 and J2.

The $Fe_{23}Zr_6$ phase was not found in HT M1 to M3 and J1 to J2, nor in the as-cast ones.

As shown in Table 2, alloys H and L which were manufactured with procedure (2) showed the presence of the $Fe_{23}Zr_6$ compound. Despite the high degree of purity of the materials the $Fe_{23}Zr_6$ phase was found in alloy H. However, this phase was not found in samples M1 to M3 and J1 to J2, which were manufactured by procedure (1) despite the different degrees of purity of the materials. Alloys H and L as-cast and HT at 1200 ºC presented a three-phase field (Fe(α) + $Fe_{23}Zr_6$ + C15) (Figure 2). As an example, Figure 3 shows the XRD pattern of alloy H.

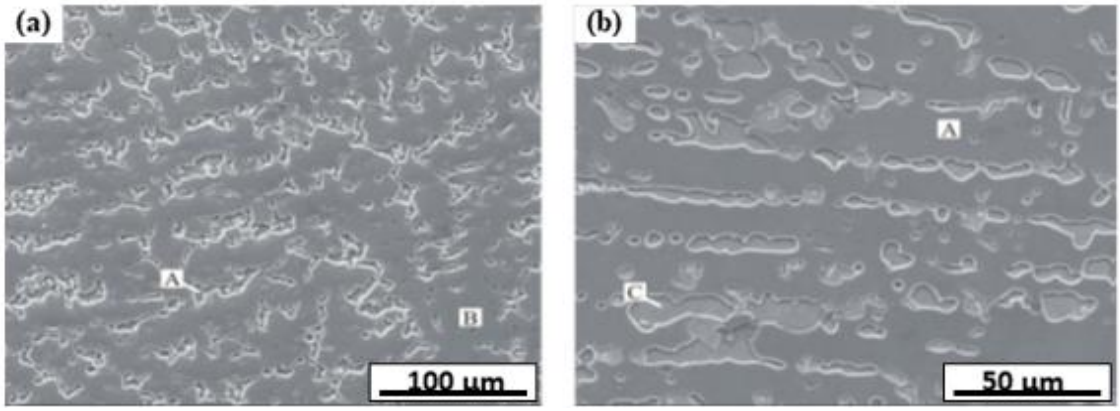

Figure 1. Secondary electron SEM images of HT samples (a) J1 and (b) J2. Identified phases: A = Fe(α), B = Fe_2Zr(C15), C = Fe_2Zr(C36).

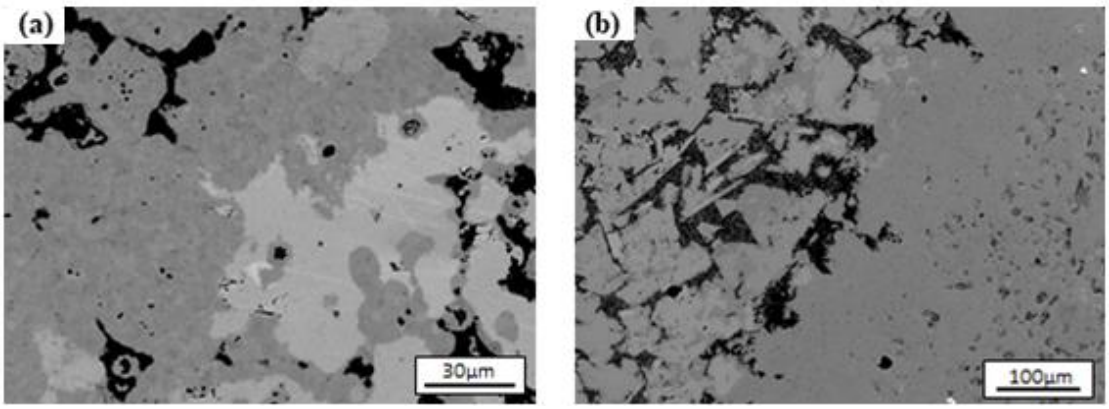

Figure 2. Back scattered electron SEM images of HT samples (a) H and (b) L. Identified phases: Fe (dark), $Fe_{23}Zr_6$ (dark grey) and C15 (grey).

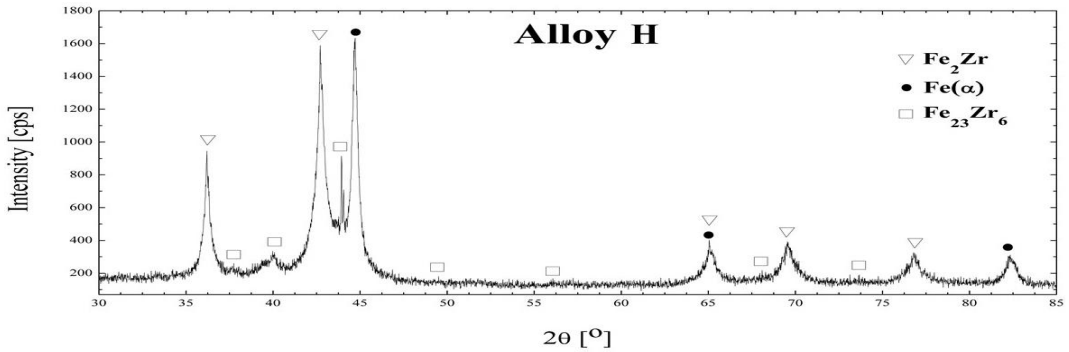

Figure 3. XRD pattern measured in alloy H heat treated at 1200 °C for 10 h.

DISCUSSION

The above mentioned C36 compound, which was found in J2 alloy, has been identified as a Laves phase with $MgNi_2$ type hexagonal crystal structure. However, the Laves C36 phase exists at higher temperature in the binary Fe-Zr phase diagram (between 1240 ºC and 1345ºC [6]). But, according to Savidan et al. [12], it would be a ternary extension of the binary C36 phase stabilized at lower temperatures by Sn substitution. Similarly, the addition of Nb generates the same phase at 700 ºC [8] and 800 °C (M1 to M3 alloys) in the Fe-Nb-Zr system.

Results of the present work at 800 ºC resemble those proposed by Liang et al. [9] at 700 °C. The main discrepancy is related to the homogeneity domain of phases C14, C15 and C36 and that the $Fe_{23}Zr_6$ phase was not found [15]. In alloys M1 to M3, raw materials of higher purity than references [7-10] and similar purity to

Yang et al. [11] were used. Also, a Ti-50at%Zr getter was melted prior to sample melting in order to reduce the contamination of oxygen and the tube was filled to the heat treatment with argon gas. The samples were heat treated at 800 ºC for 3720 hours, but the $Fe_{23}Zr_6$ phase was not found.

Huang et al. [10] heat treated alloys with large amounts of Cu(41%-46.5%) for 4 days at 1100 °C and one sample with 5 %Cu for 60 days at the same temperature. They did not report the use of getter but they put the alloys into quartz capsules, evacuated and backfilled with argon gas. Then, they found the $Fe_{23}Zr_6$ phase. Yang et. al. [11] did not melt a titanium getter and did not fill the tube with argon gas. They found the $Fe_{23}Zr_6$ phase after a heat treatment of 24 hours at 1200 °C, but it was not possible in the HT at 800 °C during 160 h.

Alloys J1-J2 were made of raw materials of high purity, a vacuum better than 10^{-4} Pa and purged with high purity argon and heat treated at 1100ºC for 60 days. However, the $Fe_{23}Zr_6$ phase was not found. Instead, the same amount of time was enough to produce the peritectic reaction for $Cu_5Fe_{85}Zr_{10}$ alloy used by Huang et al. [10]. Besides, for alloys with large amounts of Cu (41 % - 46.5 %), a heat treatment for only 4 days at 1100ºC was enough to find the $Fe_{23}Zr_6$ compound. Despite this, because the oxygen-content detected by EPMA in the $Fe_{23}Zr_6$ phase in all samples of Huang et al. was very low (in disagreement with Stein et al. [7]), it is not possible to ensure that the non-use of the getter or the contamination of the samples with oxygen during the heat treatment are responsible for the formation of the $Fe_{23}Zr_6$. Moreover, St. John [16] concluded that the peritectic reaction is unlikely to occur at the peritectic temperature (Tp), as undercooling is required to create the necessary conditions. Besides, the peritectic reaction may occur at temperatures below Tp or even not take place. Also, St. John and Hogan [17] suggest that peritectic systems can be classified on the basis of phase diagram shape and, in the Fe-Zr system, the peritectic shape corresponds to a C-type, the least favorable situation for the transformation to occur in their classification. That is to say, it is nearly a lineal compound and it is close to a high temperature eutectic reaction. Then, like the $Fe_{23}Zr_6$ compound was not found in the as-cast samples, according to St. John and Hogan [16-17], it was expected that phase $Fe_{23}Zr_6$ was not found in HT samples.

Taking into account all of the above, H and L alloys were manufactured with procedure (2) with the purpose to get a very slow cooling speed. Unlike alloys M1-M3 and J1-J2, in samples H and L the presence of the $Fe_{23}Zr_6$ compound was found in addition to Fe(α) and C15 phases (Fig. 3). Also, the micrographs of alloys H and L heat treated at 1200 °C show a large amount of $Fe_{23}Zr_6$ phase, opposite to what was found by Stein et al. [7] (diameters of 5-10 µm, in some cases up to 20 µm), Tang et al. [8] and Huang et al. [10]. Unfortunately, Liang et al. [9] did not show a micrograph with the $Fe_{23}Zr_6$ phase.

CONCLUSIONS

The $Fe_{23}Zr_6$ phase was not found in the binary and ternary alloys manufactured with procedure (1). Then, the cooling kinetics during the manufacture of the alloys was modified, achieving a slow cooling as proposed by others authors (Granovsky and Arias). The experimental evidence collected from the characterization of as-cast and heat-treated alloys manufactured with two different melting procedures would indicate the $Fe_{23}Zr_6$ phase is an equilibrium phase in the Fe-Zr binary system, independently of the amount of oxygen and impurity of the raw materials.

ACKNOWLEDGEMENTS

This work was supported by two CONICET Scholarships and CIUNT-UNT through Project PIUNT E649/1. The authors are thankful to Dr. Daniel Vega (CAC, CNEA), Dra. Gladys Nieva and Dr. Julio Guimpel (CAB, CNEA) and Dr. Gustavo Castellano (LAMARX, FaMAF, UNC).

REFERENCES

[1] V. N. Svechnikov, A. Ts. Spektor, “The Iron-Zirconium Phase Diagram”, Proceedings of the Academy of Sciences of the USSR, Chemistry section, v.142, p.231-233 (1962). In English; TR: Dokl. Akad. Nauk SSSR, v.143, p.613-15 (1962).

[2] V. N. Svechnikov, V. M. Pan, A. Ts. Spektor, “Intermediate Phases in the Iron-Zirconium System”, Russian Journal of Inorganic Chemistry, v.8, p.1106-1109 (1963) - In English; TR: Zh. Neorg. Khim., v.8, p.2118 (1963).

[3] D. Arias, M. B. Granovsky, J. P. Abriata, “Phase Diagrams of Binary Iron Alloys”, H. Okamoto Edition, ASM International, Materials Park, v.1, p.467-472 (1993).

[4] M. Granovsky, D. Arias, “On the $ZrFe_2 + L \rightarrow Fe_{23}Zr_6$ peritectic transformation”, In: Anales de la Asociación Argentina de Física, v.3, p.270-272 (1991).

[5] M. Granovsky, D. Arias, “Intermetallic phases in the iron-rich region of the Zr-Fe phase diagram”, Journal of Nuclear Materials, v.229, p.29-35 (1995).

[6] D. P. Abraham, J. W. Richardson Jr, S. M. McDeavitt, "Formation of the $Fe_{23}Zr_6$ phase in an Fe-Zr alloy", Scripta Materialia, v.37, n.2, p.239-244 (1997).

[7] F. Stein, G. Sauthoff, M. Palm, "Experimental determination of intermetallic phases, phase equilibria, and invariant reaction temperatures in the Fe–Zr system", Journal of Phase Equilibria, v.23, n.6, p.480-494 (2002).

[8] Y. Tang, C. Liao, J. Meng, J. Zhu, Q. Zhu, L. Nong, J. Liang, "Phase equilibria in the Fe-Nb-Zr ternary system at 1200°C", Rare Metals, v.32, n.2, p.201-207 (2013).

[9] J. Liang, M. Zhang, Y. Ouyang, G. Yuan, J. Zhu, J. Shen, M. Daymond, "Contribution on the phase equilibria in Zr-Nb-Fe system", Journal of Nuclear Materials, v.466, p.627-633 (2015).

[10] W. L. Huang, Y. Yu, Y. Yang, P. Wang, X.J. Liu, R. Kainuma, K. Ishida, "Experimental Investigation of Phase Equilibria in the Cu-Fe-Zr Ternary System", Journal of Phase Equilibria and Diffusion, v.34, p.438-446 (2013).

[11] Y. Yang, L. Z. Tan, H. B. Bei, J. T. Busby, "Thermodynamic modelling and experimental study of the Fe-Cr-Zr system", Journal of Nuclear Materials, v.441, p.190–202 (2013).

[12] J. C. Savidan, J. M. Joubert, C. Toffolon-Masclet, "An experimental study of the Fe-Sn-Zr ternary system at 900 °C", Intermetallics, v.18, n.11, p.2224-2228 (2018).

[13] N. Nieva, C. Corvalan, M. J. Jimenez, A. Gomez, C. Arreguez, J. M. Joubert, D. Arias, "Phase diagram of the Fe-Sn-Zr system at 800°C", Journal of Nuclear Materials, v.487, p.186-191 (2017).

[14] N. Nieva, M. R. Tolosa, C. Corvalan, D. Arias, "Diagrama de fases experimental Fe-Sn-Zr. Nuevos resultados del corte isotérmico de 800 °C", Revista Materia, v.23, n.2 (2018).

[15] C. Arreguez, M. R. Tolosa, D. Arias, C. Corvalan, N. Nieva, "Experimental Phase diagram of the Fe corner in the Fe-Nb-Zr system at 800 ºC", Journal of Nuclear Materials, v.509, p.158-161 (2018).

[16] D. H. St John, "The peritectic reaction", Acta Metallurgica et Materialia, v.38, n.4, p.631-636 (1989).

[17] D. H. St John, L. M. Hogan, "A simple prediction of the rate of the peritectic transformation", Acta Metallurgica, v.35, n.1, p.171-174, (1987).